Available online at www.sciencedirect.com

SciVerse ScienceDirect

Procedia Environmental Sciences 19 (2013) 168 – 177

Procedia Environmental Sciences

Four Decades of Progress in Monitoring and Modelling of Processes in the Soil-Plant-Atmosphere System: Applications and Challenges

Modelling Vegetation Patterns in Semiarid Environments

Salvatore Manfreda[a,]*, Teresa Pizzolla[a], Kelly K. Caylor[b]

[a] *School of Engineering, University of Basilicata, via dell'Ateneo lucano, 10, Potenza, 85100, Italy*
[b] *Department of Civil and Environmental Engineering, Princeton University, Engineering Quadrangle, Princeton, NJ 08540, USA*

Abstract

The aim of this work is to deepen our understanding on the mutual relationship between climate, vegetation and soil water budget within an ecohydrological framework. To this end a coupled hydrological/ecological model is adopted to describe simultaneously soil water budget and vegetation pattern evolution in a semiarid river basin in New Mexico (USA). This basin represents an ideal area to study the properties of water-controlled ecosystems. Analyses have been carried out using a recently formulated framework for the water balance at the daily level linked with a vegetation model for the description of the spatial organization of vegetation. Using this approach, we identified the dynamic water stress of vegetation during the growing season, taking into account effects of morphology on the spatial distribution of solar radiation and the initial soil moisture condition at the beginning of the growing season. Several different variants of the vegetation model have been tested with the aim to identify the main drivers for the spatial organization of the vegetation. Results clearly show that the observed vegetation patterns emerge from the minimization of water stress and the maximization of water use.

Selection and/or peer-review under responsibility of the Scientific Committee of the conference

keywords: vegetation patterns, soil water balance, potential evapotranspiration, vegetation water stress.

1. Introduction

The complex interaction between climate, soil and vegetation makes it difficult to define specific mechanisms of ecohydrological optimization of spatial structure of vegetation. As a consequence, a significant number of scientists are focusing on the development of models able to predict the formation

* Corresponding author. Tel.: +39 0971 205140; fax: +39 0971 205160.
E-mail address: salvatore.manfreda@unibas.it - web: www2.unibas.it/manfreda

1878-0296
Selection and/or peer-review under responsibility of the Scientific Committee of the Conference
doi:10.1016/j.proenv.2013.06.019

of spatial patterns of vegetation. In semiarid environment, water is the driving force in shaping the vegetation distribution and composition [1; 2; 3]. For this reason, theories of self-organization are often invoked to explain the emergent patterns [4; 5; 6; 7; 8]. Other mathematical models incorporate the physical mechanism of symmetry-breaking instabilities to recreate the diverse set of spatial patterns observed in these environments [9].

There is a clear need to develop conceptual models that are capable of interpreting and predicting spatial pattern formation in dryland (and similar ecosystems), as well as metrics for assessing optimization or organization of patterns. Vegetation patterns on the landscape are mainly a function of the availability of light [10; 11], nutrients [12; 13; 14], and soil moisture [15; 16] that support plant growth, and other environmental conditions, such as temperature and snow, that determine the timing and length of the growing season [17]. Therefore, plant types and patterns are under the influences of climate at the regional scale, and soil properties and topography at the local scale [18; 19; 20].

To better understand how physical and biological processes influence vegetation patterns, it is important to investigate the interaction between climate, soil and vegetation. Ecohydrological models represent a useful tool to describe the effects of climate on natural ecosystems and landscape. Among others, Caylor et al. [21] recently proposed an interesting model where vegetation patterns are defined according to two main factors: soil water stress [22] and river basin morphology. In the present study, we explored the potential of this model using different options of the replacement strategies of different plants. These changes have been made with the specific aim to identify the driving principle for vegetation patterns organization. Moreover, in order to provide a more careful description of soil moisture dynamics, we incorporated the effect of river basin morphology on the incident solar radiation and the effect of seasonality in the proposed framework.

2. Description of the case study

The study area is the Upper Rio Salado basin located near the Sevilleta Long-term Ecological Research (LTER) site in central New Mexico (Fig. 1). This represents an ideal area to study water-controlled ecosystems in which soil moisture plays a critical role. The basin is characterized by a marked heterogeneity in vegetation composition that may be influenced by the basin topography.

The basin covers an area of 464 km^2 and its elevation ranges from 1985 m above sea level (a.s.l) to 2880 m a.s.l. It contains three different soil textures: loam and silty loam, in the upper part of the basin, and sandy-loam along the channel network. The composition of vegetation cover can be distinguished in three different plant functional types: grassland (25.4%), shrubland (28%), and forest (45.7%). A small fraction of the basin (<1%) is represented by bare soil. Maps of soil texture and vegetation cover are given in Fig. 1. More detailed information about the site is available in Caylor et al. [19].

For the scope of the work, analyses are focused on the growing season in order to describe the state of plant during this phase. Rainfall and temperatures characteristics were studied by Caylor et al. [19] using the reference period 1990-2001. To this aim, the rate of rainfall, $R(t)$, is represented as a marked Poisson process of storm arrival in time with rate $\lambda(d^{-1})$, each storm having a depth h(mm), where h is modelled as an exponentially distributed random variable with mean α(mm). Both rainfall and temperature are strongly controlled by local elevation, consequently these variables were assumed spatially variable using the following relationships between elevation (x expressed in meter above the sea level) and parameters of rainfall processes (λ and α) or mean temperature estimated for the dormant and growing season.

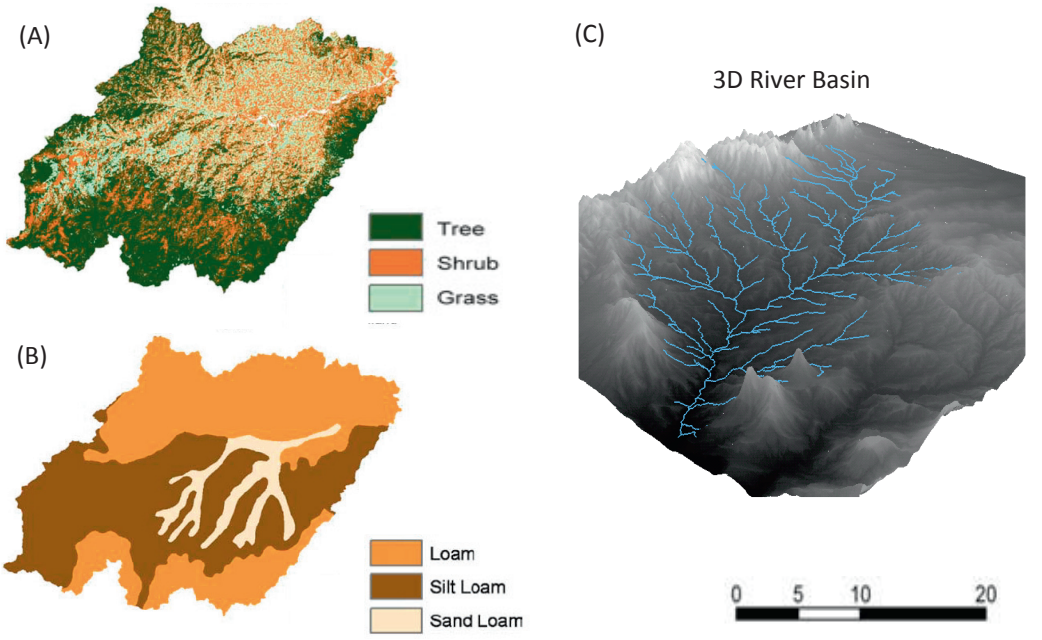

Fig. 1. Map of vegetation (A), soil texture (B) and 3D representation (C) of the Upper Rio Salado basin (New Mexico, USA).

Table 1. Functions describing the climatic parameters during the two reference periods (the dormant season from October-April and the growing season from May to September).

Dormant season	Growing season	Eq.
$\lambda = 1 * 10^{-4}\, x + 0.014$ [1/day]	$\lambda = 8 * 10^{-5} x + 0.1025$ [1/day]	(1)
$\alpha = 0.002\, x + 0.0092$ [cm/event]	$\alpha = 0.0014\, x + 2.56$ [cm/event]	(2)
$T_a = -0.0029\, x + 13.08$ [°C]	$T_a = -0.0068\, x + 33.34$ [°C]	(3)

3. Methodological approach

We investigated the influences of soil moisture, solar radiation distribution and seasonality of climatic forcing on the spatial organization of vegetation. The model adopted here describes the coupled dynamics of soil moisture and its linkage with vegetation. In particular, soil moisture dynamics are described following the approach proposed by Laio et al. [23], while the vegetation distribution is defined using the model proposed by Caylor et al. [21].

The impact of solar radiation is studied paying particular attention to the effects of basin morphology on the distribution of incoming radiation at the local scale. Basin morphology, in fact, modifies the amount of direct solar radiation, and also the amount of diffuse and reflected solar radiation received by a given point of the river basin. This influences the potential evapotranspiration that is critical in the characterization of vegetation water stress. Using the analytical model developed by Allen et al. [24], it is

possible to describe the radiation balance taking into consideration the effects of basin morphology. This approach is extremely useful to describe the spatial distribution of solar radiation and to derive the potential evapotranspiration maps during any phase of the year [25].

The other innovative aspect introduced in the present study is related to the definition of vegetation water stress, accounting for the initial soil moisture conditions at the beginning of the growing season. The initial state of the basin must necessarily be taken into account to define the dynamic water stress of vegetation in climates marked by strong seasonality. With this specific aim, the dynamic water stress has been computed using the correction factor introduced by Rodrìguez-Iturbe and Porporato [3].

3.1. Solar radiation and potential evapotranspiration

Evapotranspiration (ET) is one of the most important processes that characterize the hydrological cycle. Together with precipitation, ET represents the major water flux exchange occurring within the Earth system. In water-limited ecosystems, evapotranspiration (ET) losses can account for more than 95% of all water inputs [26]. In this context, Penman-Monteith method proved to be the most suitable in different climate contexts. Penman-Monteith method estimates the latent heat flux according to the equation (4):

$$\lambda ET_0 = \frac{\Delta(R_n - G) + \rho_a c_p \dfrac{(e_s - e_a)}{r_a}}{\Delta + \gamma\left(1 + \dfrac{r_s}{r_a}\right)}, \tag{4}$$

where λ is the latent heat of vaporization [MJ kg^{-1}]; Δ represents the slope of the saturation vapour pressure curve [kPa °C^{-1}]; R_n is the net radiation [MJ m^{-2} day^{-1}]; G is the soil heat flux [MJ m^{-2} day^{-1}]; ρ_a is the mean air density at constant pressure [kg m^3]; c_p is the specific heat of the air [kJ kg^{-1}°C^{-1}]; e_s is the saturation vapour pressure [kPa]; e_a is the actual vapour pressure [kPa]; r_a is the aerodynamic resistance [m s^{-1}]; r_s is the surface or canopy resistance [m s^{-1}]; γ is the psychometric constant [kPa °C^{-1}].

To evaluate evapotranspiration, it is necessary to estimate the net radiation R_n and soil heat flux, G. R_n can be derived from the soil radiation balance:

$$R_n = R_G(1 - \alpha) - \varepsilon_s \sigma T_s^4 + \varepsilon_a \sigma T_a^4, \tag{5}$$

where R_G is the global solar radiation [MJ m^{-2} day^{-1}] reaching the earth, which is the sum of the direct radiation, R_{dir}, of diffuse radiation, R_{dif}, and of reflected radiation from the surrounding land, R_{rif}; α is the albedo [%]; $\varepsilon_s \sigma T_s^4$ [MJ m^{-2} day^{-1}] represents the earth longwave radiation; $\varepsilon_a \sigma T_a^4$ [MJ m^{-2} day^{-1}] represents the atmospheric longwave radiation; ε_s is the earth emissivity coefficient [%]; ε_a is the atmospheric emissivity coefficient [%]; σ is the Stefan-Boltzmann constant [MJ m^{-2} K^{-4} day^{-1}]; T_s is the earth surface temperature [K] and T_a is the atmospheric temperature [K]. Generally, the atmosphere temperature and the earth temperature are assumed coincident. In such case, the net emissivity, ε, is equal to the difference between the atmospheric emissivity and surface emissivity. In this way, the equation 5 can be simplified:

$$R_n = R_G(1 - \alpha) - \varepsilon \sigma T^4. \tag{6}$$

The soil heat flux, G, is assumed to be equal to 10% of net radiation [27].

Allen et al. [24] proposed an analytical solution for the computation of daily global radiation over an inclined surface. This algorithm accounts for local slope and aspect of surface and evaluates all components of global solar radiation (direct, diffuse and reflected). These components of the incident solar radiation are computed starting from the extraterrestrial solar radiation, R_a, which is a function of solar incidence angle (θ). Its value at the daily time scale can be estimated integrating the solar incident angle between two limit values at sunrise and sunset.

$$R_a = \frac{G_{SC}}{d^2} \int_{\omega_1}^{\omega_2} cos(\theta)\, d\omega, \tag{7}$$

where G_{SC} is the solar constant (1367 Wm^2); d^2 is the inverse relative distance earth-sun; ω is the sun hour angle.

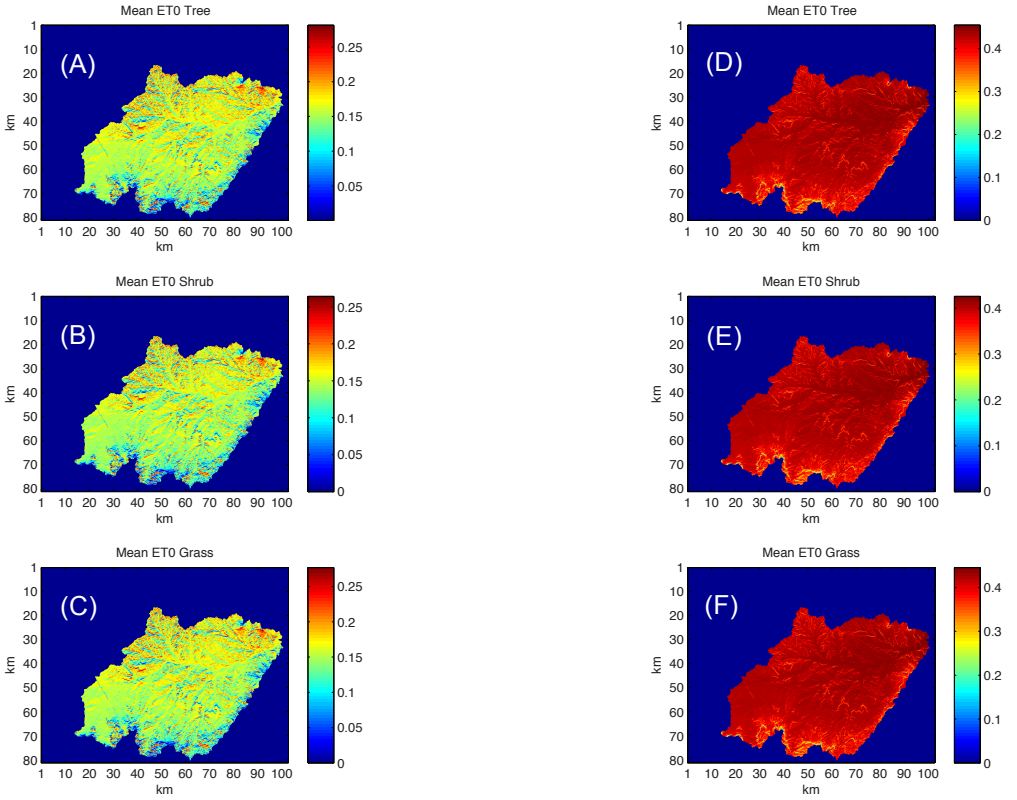

Fig. 2. Potential evapotranspiration [cm/day] computed using the Penman-Monteith equation, where the solar radiation is estimated with the algorithm proposed by Allen et al. [24] during the dormant period [October-April] (A, B, C) and the growing season [May-September] (D, E, F) for the three different PFT (tree, shrub and grass).

Following the approach proposed by Allen et al. [24], we defined the spatial patterns of potential evapotranspiration estimated on the mean climatic characteristics (described in Table 1) for both the dormant [October-April] and the growing season [May-September]. The patterns of potential

evapotranspiration, estimated during the two reference periods, are given in Fig. 2, where one may appreciate the strong influence of basin morphology on the distribution of solar radiation and as a consequence on the potential evapotranspiration. The observed variability tends to be even more significant during the dormant phase.

3.2. Relative soil saturation and its effects on vegetation water stress

In this section, we provide a brief summary of the concepts used to formulate the dynamic water stress index based on the probabilistic structure of soil moisture proposed by Laio et al. [23]. The concept is derived from the so-called "static" water stress ζ that measures the state of stress of the plants as a function of the relative saturation of soil, $s(t)$, [22]:

$$\zeta(t) = \begin{cases} 1 & if \quad s(t) \le s_w \\ \left[\dfrac{s^* - s(t)}{s^* - s_w}\right]^q & if \quad s_w \le s(t) \le s^* \\ 0 & if \quad s(t) > s^* \end{cases} \tag{8}$$

where the exponent q accounts for the non-linear relationship between plant stress and soil water content, s_w is the relative soil saturation at the wilting point and $s*$ at the point in which plant start to close stomata.

The static stress does not account for the temporal dynamic of soil moisture, for this reason Porporato et al. [22] introduced the two variables: T_ξ the length of the time intervals in which the soil moisture is below a threshold ξ (in the present case represented by $s*$), and the number, $\overline{n}_\xi$, of such intervals.

These metrics allow the definition of the average dynamic water stress under steady state conditions:

$$\bar{\theta} = \begin{cases} \left(\dfrac{\bar{\zeta}' \, \overline{T}_{s^*}}{K T_{seas}}\right)^{\frac{1}{\sqrt{\overline{n}_{s^*}}}} & \bar{\zeta}' \, \overline{T}_{s^*} < \mathrm{K} T_{seas} \\ 1 & \text{elsewhere} \end{cases} \tag{9}$$

where $\overline{\zeta}'$ is the average static water stress during the periods of stress conditions; K is an index of plant resistance to water stress; T_{seas} is the length of growing season; $\overline{T}_{s^*}$ is length of the time intervals in which the relative soil saturation is below $s*$, and n_{s^*} is the number of such intervals during the growing season.

Given the seasonal fluctuations observed in both rainfall and potential evapotranspiration, the dynamic water stress has been rescaled using a correction factor that takes into account the effects of initial conditions of soil. With this purpose, the initial soil moisture conditions have been assumed equal to the mean relative saturation of soil, defined by using the stochastic model proposed by Laio et al. [23], during the dormant season. The distribution of the mean soil saturation during the dormant season is depicted in Fig. 3 for the three different plant functional types (PFT) studied herein.

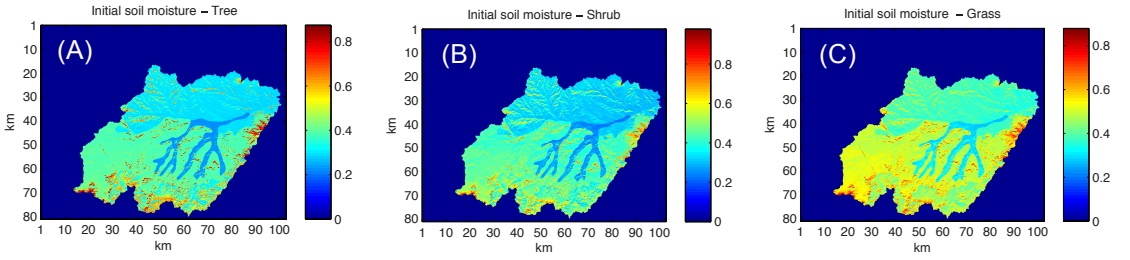

Fig. 3. Mean value of soil saturation for the three PFT (tree, shrub and grass) during the dormant period in the Upper Rio Salado basin.

In order to account for the initial state of the soil moisture, we used the correction factor proposed by Rodrìguez-Iturbe and Porporato [3] that rescales the dynamic water stress according to the mean first passage $\overline{T}_{\langle s\rangle}(s_o)$ (in days) of the stochastic process between the initial condition, s_0, and the steady-state mean relative soil saturation, $\langle s\rangle$. The equation adopted is the following:

$$\bar{\theta}' = \left(\frac{T_{seas} - \overline{T}_{\langle s\rangle}(s_o)}{T_{seas}}\right)\bar{\theta} \tag{10}$$

For any initial condition s_0 above the steady-state mean relative soil saturation $\langle s\rangle$, it is possible to determine the mean first passage $\overline{T}_{\langle s\rangle}(s_o)$ (in days) of the stochastic process between s_0 and $\langle s\rangle$, which we use to rescale the dynamic water stress experienced by vegetation. This reformulation of the dynamic water stress represents the stress experienced by vegetation during the portion of the growing season not influenced by the transient dynamics associated with an initial condition when water is readily available.

The definition of $\overline{T}_{\langle s\rangle}(s_o)$ is given by [3]:

$$\overline{T}_{\langle s\rangle}(s_o) = \overline{T}_{s_o}(s_o) - \overline{T}_{\langle s\rangle}(\langle s\rangle) + \frac{1}{\nu(\langle s\rangle)} - \frac{1}{\nu(s_o)} + \gamma\int_{\langle s\rangle}^{s_o}\left(\frac{1}{\nu(u)} - \overline{T}_u(u)\right)du. \tag{11}$$

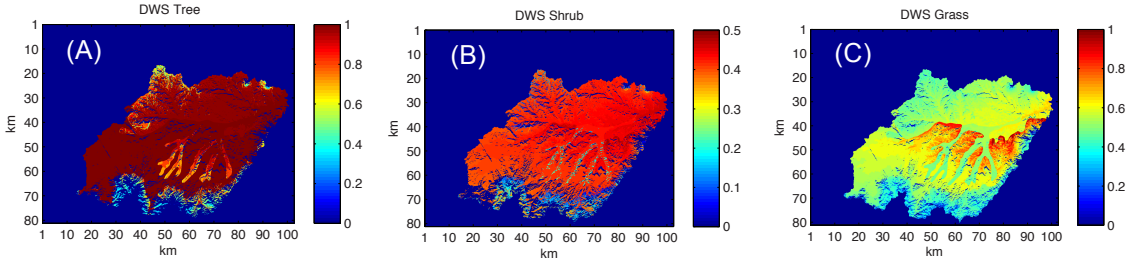

Fig. 4. Dynamic water stress during the growing season computed using as initial condition the mean soil saturation of the dormant period given in Fig. 3 and the potential evapotranspiration depicted in Fig. 2.

Maps of the dynamic water stress computed with equation 9 are depicted in Fig. 4 for each plant type. In this figure, one may appreciate the strong irregularity of these spatial patterns. In general, shrub and grass experience a lower dynamic water stress, while trees have the higher values of stress with the exceptions of sites at the higher elevation and in north facing slopes where $\bar{\theta}'$ may reach zero values.

3.3. Vegetation model

Space-time variability of soil moisture has important implications on plant growth and stress leading to patterns formation in dryland ecosystems [28; 29; 30]. The impact of plant water stress on the organization of vegetation patterns can be explored by using the dynamic water stress and the plant transpiration.

The hypothesis of feasible optimality is explored using four simple cellular automata approaches to model the steady state conditions of a vegetation mosaic, initiated from a random condition containing 1/3 each of trees, shrub and grass. In each model, the initial random vegetation mosaic is modified through the iteration of local interactions that occur between adjacent locations. These interactions are defined such that vegetation replacement can occur, at a randomly chosen location in an adjacent location, according to a replacement probability defined using the different hypothesis. In particular, the replacement probabilities (P) adopted combine both the dynamic water stress ($\bar{\theta}'$) and the plant transpiration (T). The schemes proposed are the following:

i) $P=(1-\bar{\theta}_1'/(\bar{\theta}_1'+\bar{\theta}_2'))$ with the condition that the replacement occur only if $\bar{\theta}_1' < \bar{\theta}_2'$;

ii) $P=(1-\bar{\theta}_1'/(\bar{\theta}_1'+\bar{\theta}_2'))$ with the condition that the replacement occur only if $T_1 < T_2$;

iii) $P=(1-\bar{\theta}_1'/(\bar{\theta}_1'+\bar{\theta}_2'))((T_1-T_2)/T_1)$;

iv) $P=(1-\bar{\theta}_1'/(\bar{\theta}_1'+\bar{\theta}_2'))(T_1/(T_1+T_2))$.

The application of the described models produced the vegetation patterns depicted in Fig 5. Results show that basin morphology significantly affects the spatial distribution of vegetation in all cases. Among all considered cases, the second and third schemes (see Fig. 5 B and C) provide spatial patterns that replicate more closely the actual distribution of vegetation in the Rio Salado basin (see Fig.1.A). These two algorithms tend to distribute vegetation within the landscape minimizing dynamic water stress and maximizing vegetation water use. These two mechanisms together may be considered as the driving principles for the organization of vegetation in semi-arid environment [see 4].

4. Conclusion

In the present work, we present some preliminary results on the use of an ecohydrological model based on the soil moisture scheme proposed by Laio et al. [23], where the impact of morphology was incorporated by the use of climatic parameters related to the local elevation and adopting an analytical model for the estimation of incident solar radiation and potential evapotranspiration, accounting for the effect of local slope and exposure [24]. The soil water balance model was coupled with a vegetation model, where different algorithms have been tested for the simulation of vegetation patterns. Among all

analysed schemes, the algorithm that seems to explain the actual structure of vegetation observed in the Upper Rio Salado basin is the one that tend to minimize dynamic water stress and maximize vegetation water use.

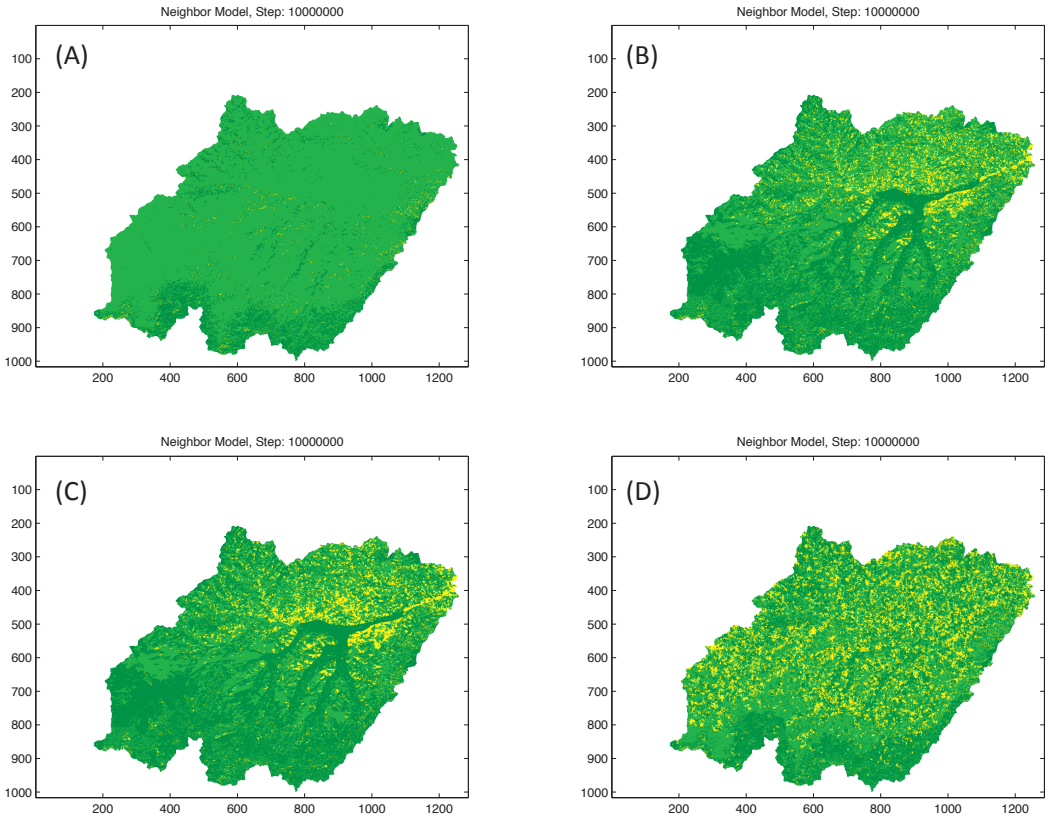

Fig. 5. Vegetation map obtained with the vegetation model using a four different replacement probability: A) $P=(1-\bar{\theta}_1'/(\bar{\theta}_1'+\bar{\theta}_2'))$ with the condition $\bar{\theta}_1' < \bar{\theta}_2'$; B) $P=(1-\bar{\theta}_1'/(\bar{\theta}_1'+\bar{\theta}_2'))$ with the condition $T_1 < T_2$; C) $P=(1-\bar{\theta}_1'/(\bar{\theta}_1'+\bar{\theta}_2'))((T_1-T_2)/T_1)$; D) $P=(1-\bar{\theta}_1'/(\bar{\theta}_1'+\bar{\theta}_2'))(T_1/(T_1+T_2))$.

References

[1] Rodrìguez-Iturbe I, D'Odorico P, Porporato A, Ridolfi L. On the spatial and temporal links between vegetation, climate, and soil moisture, *Water Resour Res* 1999, **35**(12), 3709-3722.

[2] Smit G, and Rethman N. The inuence of tree thinning on the soil water in a semi-arid savanna of southern africa, *J Arid Environ* 2000, **44**:41-59.

[3] Rodrìguez-Iturbe I., and Porporato A. *Ecohydrology of Water-Controlled Ecosystems: Soil Moisture and Plant Dynamics*, Cambridge Univ. Press, Cambridge, UK 2005.

[4] Caylor KK, Scanlon TM, Rodrìguez-Iturbge I. Ecohydrological optimization of pattern and processes in water-limited ecosystems: A tradeoff-based hypothesis, *Water Resour Res* 2009, **45**, W08407, doi:10.1029/2008WR007230.

[5] Eagleson PS. Ecological optimality in water-limited natural soil-vegetation systems. 1. Theory and hypothesis, *Water Resour Res* 1982, **18**, 325-340.

[6] Huang C, Marsh SE, McClaran M, and Archer S. Postfire stand structure in a semiarid savanna: cross-scale challenges estimating biomass, *Ecol Appl* 2007, **17**: 1899–1910.
[7] Kerkhoff AJ, Martens SN, Shore GA, and Milne BT. Contingent effects of water balance variation on tree cover density in semiarid woodlands, *Global Ecol Biogeogr* 2004, **13**:237–246.
[8] Schymanski SJ, Sivapalan M, Roderick ML, Beringer J, and Hutley LB. An optimality-based model of the coupled soil moisture and root dynamics, *Hydrol Earth Syst Sci* 2008, **12**: 913–932.
[9] Borgogno F, D'Odorico P, Laio F, and Ridolfi L. Mathematical models of vegetation pattern formation in ecohydrology, *Rev Geophys* 2009, **47**, RG1005.
[10] Ricard JP, and Messier C. Abundance, growth, and allometry of red raspberry (Rubus idaeus L.) along a natural light gradient in a northern hardwood forest, *For Ecol Manage* 1996, **81**: 153–160.
[11] Martens SN, Breshears DD, Meyer CW. Spatial distributions of understory light along the grassland/forest continuum: effects of cover, height, and spatial pattern of tree canopies, *Ecol Modell* 2000, **126**: 79–93.
[12] Tilman D. Secondary succession and the pattern of plant dominance along experimental nitrogen gradients, *Ecol Monogr* 1987, **57**:189–214.
[13] Lejeune O, Tlidi M, Couteron P. Localized vegetation patches: A self-organized response to resource scarcity, *Phys Rev E* 2002, **66,** 010901(R).
[14] Rietkerk M, Dekker SC, de Ruiter PC, van de Koppel J. Self-organized patchiness and catastrophic shifts in ecosystems, *Science* 2004, 305, 1926– 1929.
[15] Klausmeier A. Regular and irregular patterns in semiarid vegetation, *Science* 1999, 284, 1826–1828.
[16] Couteron P, and Lejeune O. Periodic spotted patterns in semiarid vegetation explained by a propagation-inhibition model, *J Ecol* 2001, 89, 616–628.
[17] Myneni RB, Nemani RR, Running SW. Estimation of global leaf area index and absorbed par using radiative transfer models, *IEEE Trans Geosci Remote Sens* 1997, **35**, 1380–1393.
[18] Larcher W. *Physiological plant ecology*, Springer, 1995.
[19] Caylor KK, Manfreda S, Rodrìguez-Iturbe I. On the coupled geomorphological and ecohydrological organization of river basins, *Adv Water Resour* 2005, **28**(1):69-86.
[20] Manfreda, S., Ecohydrology: a new interdisciplinary approach to investigate on climate-soil-vegetation interactions, *Ann Arid Zone* 2009, **48**(3 & 4), 219-228.
[21] Caylor KK, Scanlon TM, Rodríguez-Iturbe I. Feasible optimality of vegetation patterns in river basin, *Geophys Res Lett* 2004, **31**, L13502, 4.
[22] Porporato A, Laio F, Ridolfi L, Rodrìguez-Iturbe I. Plants in water-controlled ecosystems: active role in hydrological processes and response to water stress - III. Vegetation water stress, *Adv Water Resour* 2001, **24**(7):725–44.
[23] Laio, F., Porporato A., Ridolfi L., and Rodrìguez-Iturbe I. Plants in water controlled ecosystems: Active role in hydrological processes and response to water stress, II. Probabilistic soil moisture dynamics, *Adv Water Resour* 2001, **24**(7), 707-723.
[24] Allen RG, Trezza R, Tasumi M. Analytical integrated functions for daily solar radiation on slopes, *Agr Forest Meteorol* 2006, **139**, 55-73.
[25] Pizzolla T, Acampora A, Manfreda S. Effetti legati alla morfologia nella stima della Radiazione Solare globale e dell'Evapotraspirazione potenziale, *L'Acqua* 2012, **2**, 45-53 (in Italian).
[26] Wilcox BP and Thurow TL. Emerging Issues in Rangeland Ecohydrology: Vegetation Change and the Water Cycle, *Rangeland Ecol Manag* 2006, **59**, No. 2, pp. 220-224.
[27] Allen RG, Pereira RS, Raes D, Smith M. *Crop evapotanspiration-Guidelines for computing crop water requirements*, Fao Irrigation And Drainage Paper 56, Roma, 1998.
[28] Lefever R, Lejeune O. On the origin of tiger bush, *Bull Math Biol* 1997, **59**(2):263–294.
[29] von Hardenberg J, Meron E, Shachak M, Zarmi Y. Diversity of vegetation patterns and desertification, *Phys Rev Lett* 2001, **8719**:198101-1–198101-4.
[30] HilleRisLambers R, Rietkerk M, van den Bosch F, Prins HHT, de Kroon H. Vegetation pattern formation in semi-arid grazing systems, *Ecology* 2001, **82**:50–61.